Séminaire Lotharingien de Combinatoire **80B** (2018)
Article #40, 12 pp.

Proceedings of the 30th Conference on Formal Power Series and Algebraic Combinatorics (Hanover)

Growth Diagrams from Polygons in the Affine Grassmannian

Tair Akhmejanov*[1]

[1]*Department of Mathematics, Cornell University, Malott Hall, Ithaca, NY 14850*

Abstract. We introduce growth diagrams arising from the geometry of the affine Grassmannian for GL_m. These affine growth diagrams are in bijection with the $c_{\vec{\lambda}}$ many components of the polygon space $\mathrm{Poly}(\vec{\lambda})$ for $\vec{\lambda}$ a sequence of minuscule weights and $c_{\vec{\lambda}}$ the Littlewood–Richardson coefficient. Unlike Fomin growth diagrams, they are infinite periodic on a staircase shape, and each vertex is labeled by a dominant weight of GL_m. Letting m go to infinity, a dominant weight can be viewed as a pair of partitions, and we recover the RSK correspondence and Fomin growth diagrams within affine growth diagrams. The main combinatorial tool used in the proofs is the n-hive of Knutson–Tao–Woodward. The local growth rule satisfied by the diagrams previously appeared in van Leeuwen's work on Littelmann paths, so our results can be viewed as a geometric interpretation of this combinatorial rule.

Keywords: growth diagram, Robinson–Schensted–Knuth correspondence, Littlewood–Richardson coefficient, Knutson–Tao–Woodward hive, promotion, evacuation

1 Introduction

The classical Robinson–Schensted correspondence is a bijection between permutations and pairs of same-shape standard Young tableaux. It was first written down in [15] by Robinson in an attempted proof of the Littlewood–Richardson rule. Schensted later rediscovered the bijection in [17] with the aim of understanding the longest increasing subsequences of a permutation, a point of view that was further generalized by Greene in [6]. Then Fomin [2] realized the bijection in terms of growth diagrams where standard Young tableaux are interpreted as saturated chains of partitions (see Figure 1). These diagrams are square arrays of vertices, each labeled by a partition, where three of the vertex labels of a unit square determine the label of the fourth, southeast vertex via Fomin's local rules.

The combinatorics of the RS correspondence was realized geometrically by Steinberg [20], Hesselink [8], and Spaltenstein [18], using the variety of flags preserved by a fixed nilpotent η, i.e. a Springer fiber. The components of this variety are indexed by standard

*ta328@cornell.edu

Young tableaux of shape equal to the Jordan type of η. Recall that the relative position of two flags is a permutation given by the Bruhat decomposition. For two generic flags f and f' in components corresponding to tableaux T and S respectively, their relative position is the permutation given by the RS correspondence. These results were clarified and extended by van Leeuwen in [11]. In particular, each partition of Fomin's growth diagram is the Jordan type of η restricted to $f_i \cap f'_j$. Hence, van Leeuwen completed this geometric interpretation of Fomin's combinatorial rules.

In a separate work [10], van Leeuwen gave a combinatorial rule that realized the symmetry of the tensor product of irreducible representations in terms of Littelmann paths. Namely, for two irreducible representations V_λ, V_μ of a semisimple Lie algebra $\mathfrak{g}$, the multiplicity $c^\nu_{\lambda,\mu}$ in $V_\lambda \otimes V_\mu = \bigoplus_\nu c^\nu_{\lambda,\mu} V_\nu$ is equal to the number of λ-dominant paths of weight $\nu - \lambda$ that are obtained by repeated application of the Littelmann path operators on a fixed path of weight μ [12]. Likewise, $c^\nu_{\mu,\lambda}$ is counted by an analogous set of paths, but with the roles of λ and μ reversed. Since $c^\nu_{\lambda,\mu}$ is equal to $c^\nu_{\mu,\lambda}$, it is natural to ask for a bijection between these two sets of paths, and such a bijection is given in [10] that gradually transforms a path via a local rule.

We show that this same combinatorial rule is related to the geometry of the affine Grassmannian. Using this rule, we construct new growth diagrams on a staircase shape that are in bijection with the components of the polygon space, the space of tuples in the affine Grassmannian that satisfy certain distance conditions. Within these affine growth diagrams we recover Fomin growth diagrams, as well as some classical bijections, including the RSK correspondence.

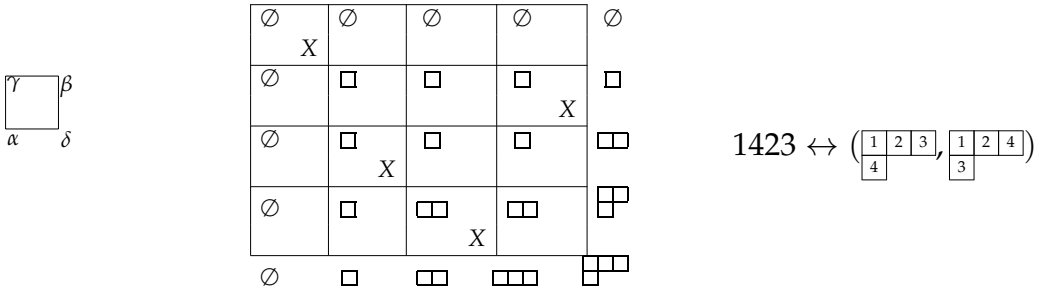

Figure 1: A Fomin growth diagram. Partitions α, β, γ of a unit square determine δ.

2 Geometry

2.1 Geometric Satake and the Polygon Space

Let $G = GL_m(\mathbb{C})$. Recall that the **dominant weights** of G are weakly decreasing sequences of m integers. The dual of a weight λ is given by negating and reversing the sequence, and is denoted λ^*. Let V_λ denote the irreducible representation corresponding to

dominant λ. Although G is not semisimple, we will say that the **minuscule weights** are the fundamental weights $\omega_i = (1, \ldots, 1, 0, \ldots, 0)$ and the dual fundamental weights $\omega_i^* = (0, \ldots, 0, -1, \ldots, -1)$ for $1 \leq i \leq m$ (where there are i many 1's and -1's respectively). For a sequence of dominant weights $\vec{\lambda} = (\lambda^1, \lambda^2, \ldots, \lambda^n)$, let $c_{\vec{\lambda}} = \dim(V_{\lambda^1} \otimes \cdots \otimes V_{\lambda^n})^G$ be **the Littlewood–Richardson coefficient**, the dimension of the invariant space.

Let $\mathcal{O} = \mathbb{C}[[t]]$ be the ring of power series and $\mathcal{K} = \mathbb{C}((t))$ the field of Laurent series. Let $Gr = G(\mathcal{K})/G(\mathcal{O})$ be the **affine Grassmannian**, an ind-variety over $\mathbb{C}$. For each dominant weight λ let $Gr(\lambda) = G(\mathcal{O})t^\lambda$ be the orbit of $G(\mathcal{O})$ in Gr where t^λ is the torus fixed point for λ. These are all of the $G(\mathcal{O})$-orbits and are distinct. Then $Gr = \sqcup Gr(\lambda)$ and $\overline{Gr(\lambda)} = \cup_{\mu \leq \lambda} Gr(\mu)$ where $\mu \leq \lambda$ under the usual dominance order of weights. The orbits of $G(\mathcal{K})$ on $Gr \times Gr$ are in bijection with orbits of $G(\mathcal{O})$ on Gr. For $p, q \in Gr$ define the **distance** to be $d(p, q) = \lambda$ if (p, q) are in the same $G(\mathcal{K})$ orbit as (t^0, t^λ). Note that $d(q, p) = \lambda^*$. One reason for the importance of the affine Grassmannian is the following theorem of Lusztig [13], Ginzburg [5], Beilinson–Drinfeld [1], and Mirković–Vilonen [14]. For general reductive groups one needs to take the Langlands dual G^L, but in our case $GL_m^L = GL_m$.

Theorem 2.1 (Geometric Satake)**.** *The tensor category of perverse sheaves on the affine Grassmannian Gr with respect to the above stratification is equivalent to the tensor category of representations of G.*

For a sequence of dominant weights $\vec{\lambda}$ consider the twisted product of orbit closures,

$$\overline{Gr(\lambda^1)} \tilde{\times} \cdots \tilde{\times} \overline{Gr(\lambda^n)} := \left\{ (g_1, \ldots, g_n) \mid d(t^0, g_1) \leq \lambda^1, d(g_i, g_{i+1}) \leq \lambda^{i+1}, 1 \leq i \leq n-1 \right\},$$

a sort of "path space" in Gr. Theorem 2.1 gives a way to construct the invariant space $(V_{\lambda^1} \otimes \cdots \otimes V_{\lambda^n})^G$ geometrically from the following convolution morphism.

$$\begin{aligned} m_{\vec{\lambda}} : \overline{Gr(\lambda^1)} \tilde{\times} \overline{Gr(\lambda^2)} \tilde{\times} \cdots \tilde{\times} \overline{Gr(\lambda^n)} &\to Gr \\ (g_1, \ldots, g_n) &\mapsto g_n \end{aligned}$$

Define the polygon space to be the projective variety $\mathrm{Poly}(\vec{\lambda}) = m_{\vec{\lambda}}^{-1}(t^0)$. The geometric Satake correspondence yields the following corollary.

Corollary 2.2. *The invariant space is isomorphic to the top homology of $Poly(\vec{\lambda})$.*

$$(V_{\lambda^1} \otimes \cdots \otimes V_{\lambda^n})^G \cong H_{top}\left(Poly(\vec{\lambda})\right)$$

Haines showed in [7, Proposition 1.8] that for GL_m, $\mathrm{Poly}(\vec{\lambda})$ is equidimensional, so as a corollary, the number of components of $\mathrm{Poly}(\vec{\lambda})$ is equal to $c_{\vec{\lambda}}$. We study the combinatorics of indexing the components when the λ^i are minuscule. Note that in this case $c_{\vec{\lambda}}$ is a rectangular Kostka number. For λ dominant minuscule, there are no dominant weights less than λ, so $\overline{Gr(\lambda)} = Gr(\lambda)$ and the inequalities above become equalities. Hence, $\mathrm{Poly}(\vec{\lambda})$ is the variety of n-gons, where a point in $\mathrm{Poly}(\vec{\lambda})$ is a tuple $(g_1, \ldots, g_{n-1}, g_n = t^0)$ satisfying the $\vec{\lambda}$ distance conditions as in Figure 2.

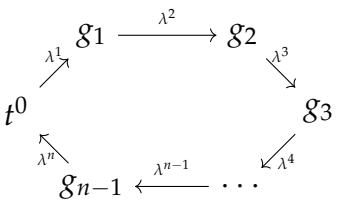

Figure 2: A point of Poly($\vec{\lambda}$)

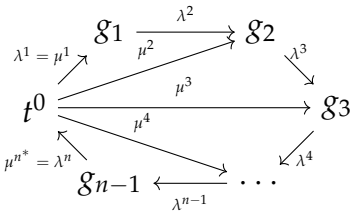

Figure 3: The fan triangulation.

2.2 Indexing Components with Affine Growth Diagrams

Assume from now on that the λ^i in $\vec{\lambda}$ are dominant minuscule. Fontaine, Kamnitzer, and Kuperberg showed in [4] that the irreducible components of Poly($\vec{\lambda}$) can be indexed by minuscule paths for $\vec{\lambda}$, namely sequences of dominant weights $\vec{\mu} = (\mu^0 = \emptyset, \mu^1, \ldots, \mu^n = \emptyset)$ such that $\mu^k - \mu^{k-1} = w \cdot \lambda^k$ for some element w in the Weyl group.

Proposition 2.3 ([4]). *Each component X of Poly($\vec{\lambda}$) has an open dense set X^o such that for all $0 \leq i \leq n$ the distance $d(t^0, g_i) = \mu^i$ is constant on X^o. The distances $\vec{\mu} = (\mu^0, \mu^1, \ldots, \mu^{n-1}, \mu^n)$ form a minuscule path for $\vec{\lambda}$, and this is a bijection between components and minuscule paths.*

Note that these distances are the ones along the edges of the fan triangulation of Figure 3. Our first observation extends this result to any extroverted triangulation. An **extroverted triangulation** is a triangulation of the n-gon such that each triangle contains an external edge (see Figure 4). Fix an extroverted triangulation τ and order its interior edges $(e_2, \ldots, e_{n-2})$ so that e_i and e_{i+1} share a vertex. Choose e_1 (respectively e_{n-1}) to be one of the two external edges sharing a vertex with e_2 (respectively e_{n-2}). Define $\sigma : [n] \to [n]$ so that $\lambda^{\sigma(1)}$ labels e_1, $\lambda^{\sigma(n-1)}$ labels e_{n-1}, and $\lambda^{\sigma(i)}$ labels the edge that completes the triangle with e_{i-1} and e_i. Orient the edges so that either the tail of e_i meets the tail of e_{i-1}, or their heads meets (see Figure 8). Let $E_\tau = (e_1, \ldots, e_{n-1})$.

Proposition 2.4. *Each component X of Poly($\vec{\lambda}$) has an open dense set X^o_τ such that for every e_i in E_τ the distance μ^i along e_i is constant on X^o_τ. This induces a bijection between the components of Poly($\vec{\lambda}$) and sequences of dominant weights, $\vec{\mu} = (\mu^0 = \emptyset, \mu^1, \ldots, \mu^{n-1}, \mu^n = \emptyset)$, such that $\mu^k - \mu^{k-1} = w \cdot \lambda^{\sigma(k)}$ for some w in the Weyl group.*

For a fixed component X, taking the intersection of the open dense sets X^o_τ over all of the extroverted triangulations τ gives an open dense set on which all the distances $d(g_i, g_j)$ are constant. Call these the generic distances for the component X. Consider a

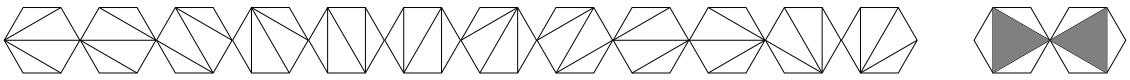

Figure 4: The 12 extroverted, and 2 non-extroverted, triangulations of the hexagon

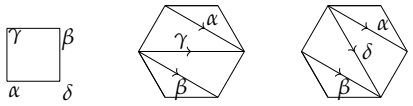

Figure 5: Dominant weights α, β, γ determine δ via one application of the local rule.

quadrilateral with two external edge in the n-gon such that the corresponding generic distances in Poly$(\vec{\lambda})$ are α, β, γ as in Figure 5 where $n = 6$. We give a local rule that given these three generic distances, determines the fourth generic distance δ, thereby performing a "quadrilateral flip".

Theorem 2.5 (Local Growth Rule)**.** *For a generic point $(g_1, \ldots, g_n)$ in a component of Poly$(\vec{\lambda})$, if the indicated distances of Figure 5 are given by α, β, γ, then $\delta = sort(\alpha + \beta - \gamma)$.*

Here weights are added component wise, so $\alpha + \beta = (\alpha_1 + \beta_1, \ldots, \alpha_n + \beta_n)$. For three dominant weights α, β, γ, the sequence $\alpha + \beta - \gamma$ need not be a weakly decreasing sequence, hence the sort operation orders the sequence of integers to make it a dominant weight.

As with Fomin growth diagrams, this rule allows us to construct growth diagrams where α, β, γ label three vertices of a unit square and determine the fourth, southeast vertex label δ according to the local rule in Theorem 2.5. We can organize the information of the generic distances of a fixed component X of Poly$(\vec{\lambda})$ into a growth diagram in a coherent manner. Consider an n-wide infinite staircase, such that each row contains $n - 1$ unit squares. We will label the vertices of the diagram with the dominant weights that are the generic distances $d(g_i, g_j)$ of X. The diagram is organized so that a path through the staircase from the left to the right diagonal, together with the weight labels along the path, corresponds to an extroverted triangulation τ, together with the generic distances of X along the edges E_τ. Begin by labelling the vertices along the left and right diagonals with the zero weight, $\emptyset$. Label the super-diagonal with $\vec{\lambda}$ periodically (see Figure 6).

Definition 2.6. An **affine growth diagram of type $\vec{\lambda}$** is a labelling of the remaining vertices by dominant weights such that the local rule is satisfied by every unit square.

Oriented extroverted triangulations correspond to paths through the staircase diagram from the left diagonal to the right diagonal as follows. An oriented extroverted triangulation can be specified by first choosing an external edge and orienting it clockwise (R) or counterclockwise (L). Then attach a doubly extroverted triangle to this edge either to the right (R) or to the left (L), orienting the internal edge of this triangle accordingly. Continue shelling on triangles to the right (R) or to the left (L) until a second doubly extroverted triangle is reached, completing the triangulation. In terms of paths through the staircase diagram, an R corresponds to a horizontal step, while an L corresponds to a vertical step. For example, the fan triangulation for $n = 6$ is encoded as

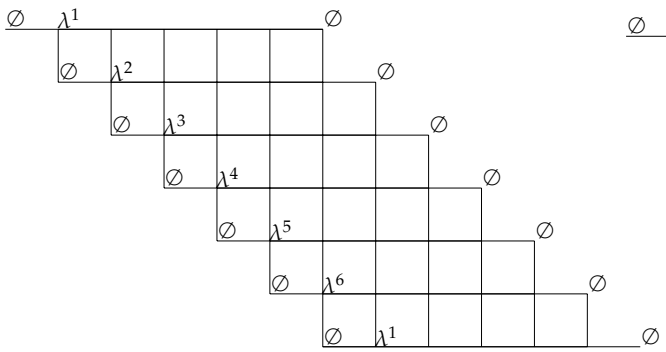

Figure 6: Empty affine growth diagram of type $\vec{\lambda} = (\lambda^1, \ldots, \lambda^6)$

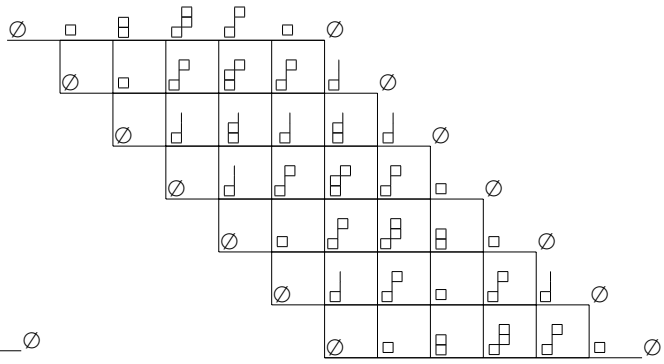

Figure 7: An affine growth diagram of type $\vec{\lambda} = (\omega_1, \omega_1, \omega_1^*, \omega_1^*, \omega_1, \omega_1^*)$

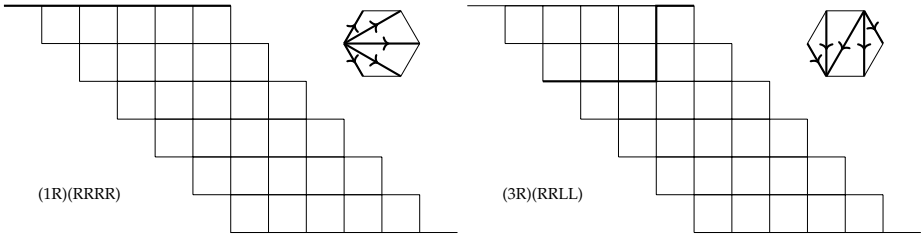

Figure 8: Extroverted triangulations correspond to paths through staircase diagram.

$(1\mathrm{R})(\mathrm{RRRR})$, and corresponds to the first line of the staircase diagram. The choice of the first external edge in the triangulation determines the row of the terminal vertex of the first step through the staircase (see Figure 8).

Fix a sequence of minuscule weights $\vec{\lambda} = (\lambda^1, \ldots, \lambda^n)$ and fix a component X of $\mathrm{Poly}(\vec{\lambda})$. Let τ be an oriented extroverted triangulation with corresponding path p_τ through the staircase. Label the vertices along the path p_τ with the corresponding generic distances of X. Since, by Proposition 2.4, the component X is determined by these generic distances along the interior edges of τ, repeated application of the local rule fills in the entire diagram, thereby determining all of the generic distances. See Figure 7 where the affine growth diagram can be filled in by starting from the vertex labels along one of the paths in Figure 8, or by starting from any other path from diagonal to diagonal.

Theorem 2.7. *Affine growth diagrams of type $\vec{\lambda}$ are in bijection with the components of $\mathrm{Poly}(\vec{\lambda})$.*

In particular, if we start with a minuscule path, i.e. the generic distances of a component along the fan triangulation, then this is the top line of the affine growth diagram. The next line of the growth diagram represents the neighboring fan triangulation. In other words, repeated application of the local rule to determine this second line rotates

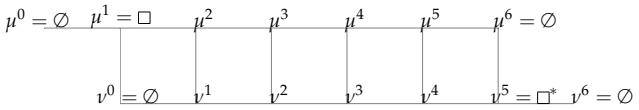

Figure 9: First row of a diagram.

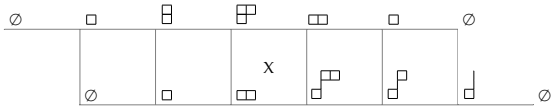

Figure 10: Example of marking the first row.

the fan triangulation. The ith line represents the distances along the ith fan triangulation. Rotating n times gets back to the initial fan triangulation, hence establishes the following proposition, which is not combinatorially obvious from the local growth rule alone.

Proposition 2.8. *Affine growth diagrams are n periodic.*

3 Classical Bijections

Suppose that the λ^i are either ω_1 or ω_1^*. In this case, there is a natural way to mark affine growth diagrams. Consider again starting with a minuscule path, the top line of an affine growth diagram, and determining the second line from repeated applications of the local rule (see Figure 9). Suppose that $\lambda^1 = \omega_1$, so that $\mu^1 = \omega_1$ as well. To compute ν^1, the local rule says to subtract one from the first row of μ^2 and sort to get ν^1. This can happen in two ways. If μ^2 had a box in the first row, then ν^1 has one fewer positive box than μ^2. If μ^2 did not have a box in the first row, then ν^1 has one more negative box than μ^2. In other words, going from μ^2 to ν^1 either removes a positive box, or adds a negative box. This relation between μ^i and ν^{i-1} continues to hold for all i. Since $\mu^1 = (1, 0, \ldots, 0)$, $\nu^0 = \emptyset$ and $\mu^6 = \emptyset$, $\nu^5 = (0, \ldots, 0, -1)$, the differences between μ^i and ν^{i-1} begin by being a removal of a positive box and finish by being an addition of a negative box, with a switch occurring somewhere in the middle. This switch is guaranteed to happen exactly once if $m \geq n/2$. Mark the unit square across which this switch occurs (see Figure 10).

Proposition 3.1. *If for all i, $\lambda^i = \omega_1$ or ω_1^*, and $m \geq n/2$, then any affine growth diagram of type $\vec{\lambda}$ has exactly one mark in every row and column, hence gives an affine permutation.*

The group $\widetilde{S_n}$ of **affine permutations** consists of bijections $f : \mathbb{Z} \to \mathbb{Z}$ such that $f(x+n) = f(x) + n$. Such an f is uniquely determined by its values on $[n]$, written as $[f(1), \cdots, f(n)]$, and called the **window** of f. From an affine permutation we obtain a classical permutation by reducing the values $[f(1), \cdots, f(n)]$ mod n. In this way, the marked squares of an affine growth diagram give a classical permutation. For example, the left diagram of Figure 12 has permutation 341265. This can be seen by moving the right, blue triangle underneath the left, red triangle to get a permutation matrix.

Proposition 3.2. *The permutation associated to an affine growth diagram is a fixed-point-free involution.*

A subset of minuscule paths are the oscillating tableaux, i.e. those consisting of weights that don't have negative parts. An **oscillating tableau** of length n is a sequence of partitions $(\mu^0 = \emptyset, \mu^1, \ldots, \mu^{n-1}, \mu^n = \emptyset)$ that differ by a box at each step. Starting with a fixed-point-free involution written into an empty staircase diagram, we give a procedure to determine the weight label at each vertex such that the result is an affine growth diagram with first row an oscillating tableaux. This procedure induces a bijection, thereby rediscovering the following Stanley–Sundaram bijection [21].

Proposition 3.3 ([21]). *For n even there is a bijection between fixed-point-free involutions of S_n and length n oscillating tableaux.*

Suppose n is even and let $\vec{\lambda} = (\omega_1, \ldots, \omega_1, \omega_1^*, \ldots, \omega_1^*)$, a sequence of $n/2$ many ω_1's followed by $n/2$ many ω_1^*'s. In this case, all minuscule paths are oscillating tableaux $(\mu^0 = \emptyset, \mu^1, \ldots, \mu^{n-1}, \mu^n = \emptyset)$ that consist of partitions that increase from $\emptyset$ to $\mu^{n/2}$ and then decrease back down to $\emptyset$. This is the same information as a pair of same-shape standard Young tableaux. In this case, the markings of the corresponding affine growth diagrams are contained in the squares indicated in Figure 11. They give a permutation in $S_{n/2}$, and this is the (transpose) RS correspondence. Furthermore, we recover Fomin growth diagrams.

Theorem 3.4. *The positive parts of the weights of the left, red, indicated square of Figure 11 give a Fomin growth diagram to the northwest, and the negative parts give a Fomin growth diagram to the southeast. The analogous statement holds for the right, blue squares.*

Hence, the RS bijection is contained in the Stanley–Sundaram bijection. In particular, starting with an oscillating tableau $\vec{\mu}$ that encodes the pair of same-shape standard Young tableaux (P, Q), suppose that (P, Q) corresponds to the permutation $\sigma = \left(\begin{smallmatrix} 1 & 2 & 3 & \cdots & k-1 & k \\ \sigma_1 & \sigma_2 & \sigma_3 & \cdots & \sigma_{k-1} & \sigma_k \end{smallmatrix}\right)$ under the RS correspondence. Then under Stanley–Sundaram, $\vec{\mu}$ corresponds to the fixed point-free-involution $\pi = \left(\begin{smallmatrix} \sigma_1 & \sigma_2 & \cdots & \sigma_{k-1} & \sigma_k & k+1 & k+2 & \cdots & 2k-1 & 2k \\ 2k & 2k-1 & \cdots & k+2 & k+1 & \sigma_k & \sigma_{k-1} & \cdots & \sigma_2 & \sigma_1 \end{smallmatrix}\right)$.

3.1 Knuth Version

In the previous subsection the λ^i were assumed to be ω_1 or ω_1^*. Dropping this assumption, affine growth diagrams can now be marked with natural numbers, the number of boxes that perform a "switch" across a unit square (see the right diagram of Figure 12). The result is an $n \times n$ symmetric matrix such that for all i either $r_i = 0$ or $c_i = 0$, where r_i, respectively c_i, denotes the sum of the entries of the ith row, respectively column, up to and including the main diagonal entry.

In [16], Roby extended the Stanley–Sundaram bijection to semistandard oscillating tableaux. A **semistandard oscillating tableau** of length n is a sequence of partitions $(\emptyset, \mu^1, \ldots, \mu^{n-1}, \emptyset)$ such that for all i, μ^i and μ^{i-1} differ by a vertical strip. As before, write such a symmetric natural-number matrix into an empty affine growth diagram.

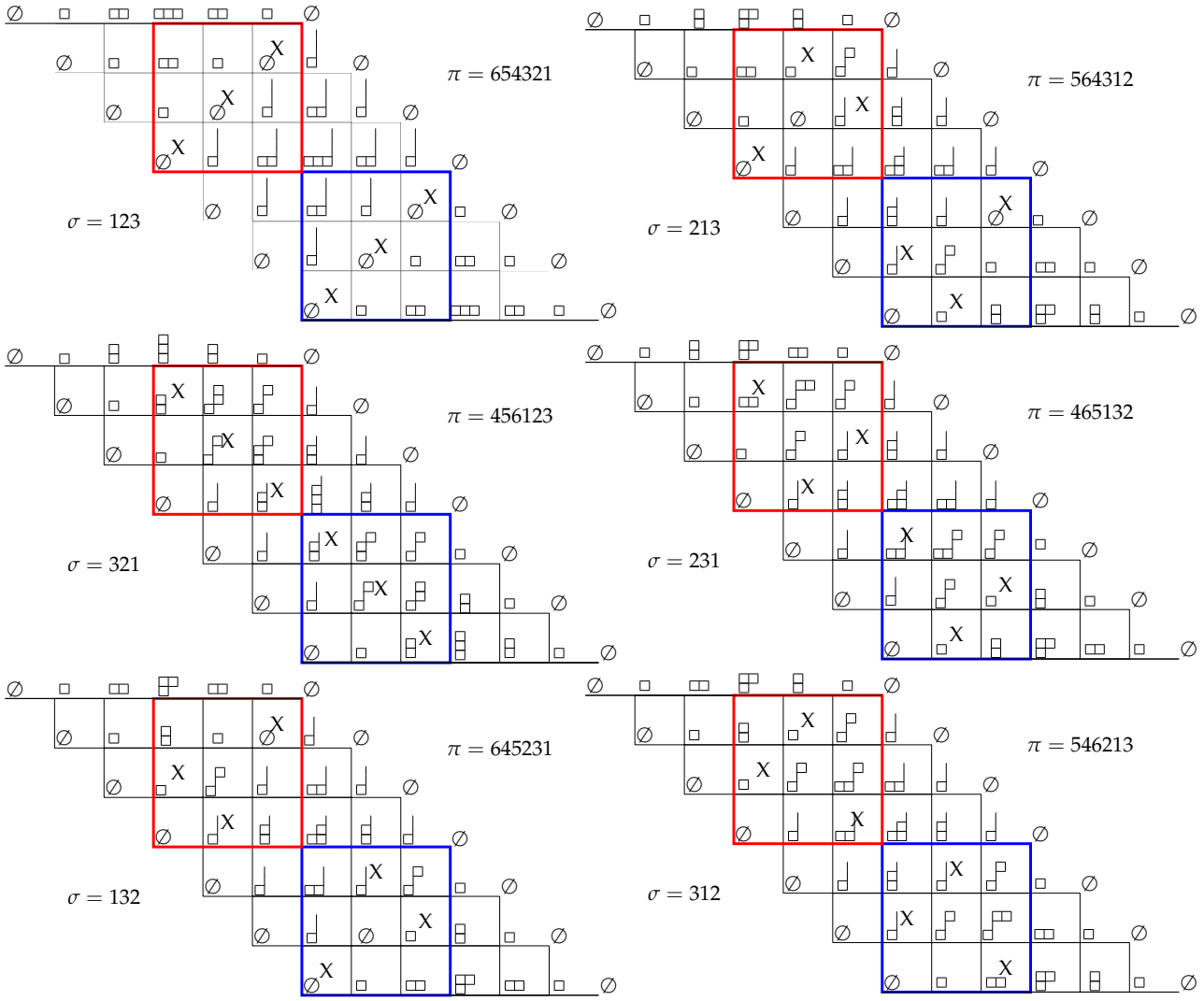

Figure 11: The six affine growth diagrams of the RS correspondence.

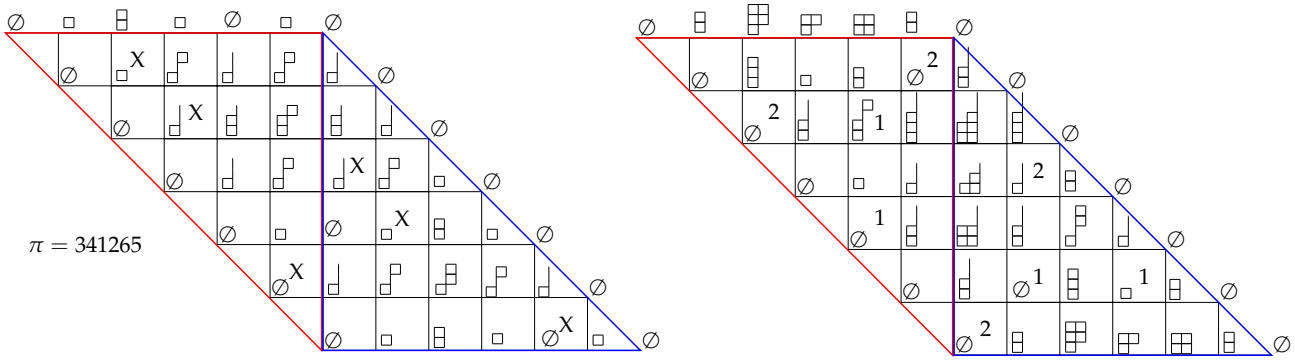

Figure 12: Standard and semistandard oscillating tableau examples.

There is a procedure to determine the weight label at each vertex such that the result is an affine growth diagram with the first row a semistandard oscillating tableau. Again, this induces a bijection, thereby rediscovering the Stanley–Sundaram/Roby bijection.

Proposition 3.5. *There is a bijection between natural-number symmetric matrices such that for all i either $r_i = 0$ or $c_i = 0$ and semistandard oscillating tableaux. Furthermore, c_i is the number of boxes added in the ith step (going from μ^{i-1} to μ^i), and r_i is the number of boxes removed.*

In the case when $\vec{\lambda} = (\omega_{i_1}, \ldots, \omega_{i_k}, \omega^*_{i_{k+1}}, \ldots, \omega^*_{i_{k+l}})$, a minuscule path is a semistandard oscillating tableau that grows for k steps to μ^k and then decreases for l steps back to the empty partition. This is the same information as a pair of (row-strict) same-shape semistandard Young tableaux with shape μ^k. Knuth [9] extended the Robinson–Schensted correspondence to give a bijection between natural-number matrices and pairs of same-shape semistandard Young tableaux. Roby [16] showed how to see the full RSK correspondence in terms of Fomin growth diagrams. As before, the (transpose) RSK bijection lives inside of the Stanley–Sundaram/Roby bijection.

Theorem 3.6. *If $\vec{\lambda}$ is as described in the previous paragraph, then the positive parts of the weights of the $k \times l$ rectangle inside of an affine growth diagram is a Fomin–Roby growth diagram to the northwest, and the negative parts give a Fomin–Roby growth diagram to the southeast.*

4 Promotion and Evacuation

We can rephrase everything in terms of dominant SL_m weights (see Figure 13). In this case a minuscule path begins at the zero weight and grows to a rectangle. Fontaine and Kamnitzer showed in [3] that, in this case, rotation of minuscule paths gives promotion of rectangular tableaux. From different geometric considerations, such diagrams were also considered by Speyer [19] in the special case that $\lambda^i = \omega_1$ for all i.

Let ∂ denote the promotion operation on tableaux computed via deflation, and ∂^* the inverse promotion operation computed via inflation, so that $\partial \circ \partial^* = \mathrm{id} = \partial^* \circ \partial$. Suppose that tableau T labels line i of the affine growth diagram. Then line $i+1$ is labeled by $\partial(T)$ and line $i-1$ by $\partial^*(T)$. The n-periodicity of the affine growth diagram recovers the n-periodicity of promotion on rectangular tableaux, $\partial^n(T) = T = (\partial^*)^n(T)$. Likewise, traversing successive vertical lines to the left is given by promotion and to the right by inverse promotion. Furthermore, the vertical line that begins where horizontal line i ends is labeled by the Schützenberger evacuation tableau $ev(T)$. The $n+i$ horizontal line is labeled by the dual evacuation procedure applied to $ev(T)$, which recovers the identity $ev^* \circ ev(T) = \partial^n(T)$, and the fact that $ev^* = ev$ in the rectangular case. We can also recover the identity $ev \circ \partial = \partial^* \circ ev$. These results are summarized in Figure 13.

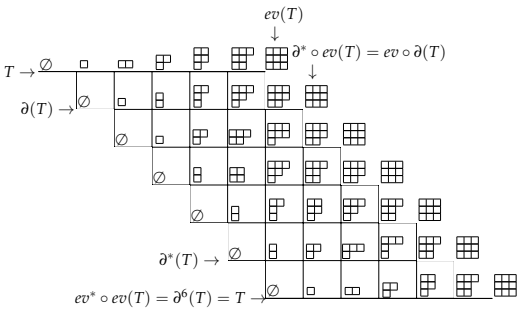

Figure 13: An SL_m growth diagram with promotion and evacuation indicated.

Acknowledgements

I would like to thank Allen Knutson for suggesting the question and for many helpful discussions, Bruce Westbury for pointing out the occurrence of the local rule in [10], and Alex Yong and David Speyer for helpful discussions.

References

[1] A.A. Beilinson and V.G. Drinfeld. "Quantization of Hitchin's fibration and Langlands' program". *Algebraic and geometric methods in mathematical physics (Kaciveli, 1993)*. Vol. 19. Math. Phys. Stud. Kluwer Acad. Publ., Dordrecht, 1996, pp. 3–7.

[2] S.V. Fomin. "The generalized Robinson-Schensted-Knuth correspondence". *Zap. Nauchn. Sem. Leningrad. Otdel. Mat. Inst. Steklov. (LOMI)* **155**.Differentsialnaya Geometriya, Gruppy Li i Mekh. VIII (1986), pp. 156–175, 195. DOI: 10.1007/BF01247093.

[3] B. Fontaine and J. Kamnitzer. "Cyclic sieving, rotation, and geometric representation theory". *Selecta Math. (N.S.)* **20**.2 (2014), pp. 609–625. DOI: 10.1007/s00029-013-0144-4.

[4] B. Fontaine, J. Kamnitzer, and G. Kuperberg. "Buildings, spiders, and geometric Satake". *Compos. Math.* **149**.11 (2013), pp. 1871–1912. DOI: 10.1112/S0010437X13007136.

[5] V. Ginzburg. "Perverse sheaves on a loop group and Langlands duality". 1995. arXiv: alg-geom/9511007.

[6] C. Greene. "An extension of Schensted's theorem". *Adv. Math.* **14** (1974), pp. 254–265. DOI: 10.1016/0001-8708(74)90031-0.

[7] T.J. Haines. "Structure constants for Hecke and representation rings". *Int. Math. Res. Not.* 39 (2003), pp. 2103–2119. DOI: 10.1155/S1073792803131285.

[8] W.H. Hesselink. "A classification of the nilpotent triangular matrices". *Compos. Math.* **55**.1 (1985), pp. 89–133. URL.

[9] D.E. Knuth. "Permutations, matrices, and generalized Young tableaux." *Pacific J. Math.* **34**.3 (1970), pp. 709–727. DOI: 10.2140/pjm.1970.34.709.

[10] M.A.A. van Leeuwen. "An analogue of jeu de taquin for Littelmann's crystal paths". *Sém. Lothar. Combin.* **41** (1998), Art.B41b, 23 pp.

[11] M.A.A. van Leeuwen. "Flag varieties and interpretations of Young tableau algorithms". *J. Algebra* **224**.2 (2000), pp. 397–426. DOI: 10.1006/jabr.1999.8070.

[12] P. Littelmann. "Characters of representations and paths in $\mathfrak{h}^*_{\mathbb{R}}$". *Representation theory and automorphic forms (Edinburgh, 1996)*. Vol. 61. Proc. Sympos. Pure Math. Amer. Math. Soc., Providence, RI, 1997, pp. 29–49. DOI: 10.1090/pspum/061/1476490.

[13] G. Lusztig. "Singularities, character formulas, and a q-analog of weight multiplicities". *Analysis and topology on singular spaces, II, III (Luminy, 1981)*. Vol. 101. Astérisque. Soc. Math. France, Paris, 1983, pp. 208–229.

[14] I. Mirković and K. Vilonen. "Geometric Langlands duality and representations of algebraic groups over commutative rings". *Ann. of Math. (2)* **166**.1 (2007), pp. 95–143. DOI: 10.4007/annals.2007.166.95.

[15] G. de B. Robinson. "On the Representations of the Symmetric Group". *Amer. J. Math.* **60**.3 (1938), pp. 745–760. URL.

[16] T.W. Roby. "Applications and extensions of Fomin's generalization of the Robinson-Schensted correspondence to differential posets". PhD thesis. Massachusetts Institute of Technology, 1991.

[17] C. Schensted. "Longest increasing and decreasing subsequences". *Canad. J. Math.* **13** (1961), pp. 179–191. DOI: 10.4153/CJM-1961-015-3.

[18] N. Spaltenstein. "The fixed point set of a unipotent transformation on the flag manifold". *Nederl. Akad. Wetensch. Proc. Ser. A* **79**=*Indag. Math.* **38**.5 (1976), pp. 452–456.

[19] D.E. Speyer. "Schubert problems with respect to osculating flags of stable rational curves". *Algebr. Geom.* **1**.1 (2014), pp. 14–45. DOI: 10.14231/AG-2014-002.

[20] R. Steinberg. "An occurrence of the Robinson-Schensted correspondence". *J. Algebra* **113**.2 (1988), pp. 523–528. DOI: 10.1016/0021-8693(88)90177-9.

[21] S. Sundaram. "On the combinatorics of representations of $Sp(2n, \mathbb{C})$". PhD thesis. Massachusetts Institute of Technology, 1986.